Mechanical Relaxation of Medical Grade UHMWPE of Different Crosslink Density as Prepared by Electron Beam Irradiation

Ulrich Göschel, Christian Ulrich

Institute for Polymer Technology (IKT), University of Stuttgart, Pfaffenwaldring 32, 70569 Stuttgart, Germany

Received 16 July 2008; accepted 6 December 2008
DOI 10.1002/app.29852
Published online 13 March 2009 in Wiley InterScience (www.interscience.wiley.com).

ABSTRACT: Dynamic mechanical thermal analysis (DMTA) has been applied on medical grade ultra high molecular weight polyethylene of different crosslink density as prepared by electron beam irradiation to probe for contributions from crosslinking as well as crystallization. The crosslinking proceeds at a crystalline structure with a crystallinity about 50%. With increasing irradiation dose from 0 to 110 kGy, the molar mass between adjacent crosslinks decreases significantly to reach 3170 g/mol at lowest, whereas the crystallite thickness changes and new thin lamellae grow at almost constant degree of crystallinity. From DMTA in the entire temperature range from −150 to +140°C and the angular frequency range from 0.6 to 135.4 Hz, three relaxation processes γ, β, and α of different temperature position and activation energy are distinguished. The corresponding chain mobility has been discussed as a sensitive discriminator for the coexisting crosslinked and lamellar phases showing the same dimension of a couple of 10 of nanometres. © 2009 Wiley Periodicals, Inc. J Appl Polym Sci 113: 49–59, 2009

Key words: electron beam irradiation; polyethylene; crosslinking; crystallization

INTRODUCTION

Because of the combination of well lubricity, impact resistance and abrasion resistance, the ultra high molecular weight polyethylene (UHMWPE) medical grade homopolymer has been accepted as an appropriate bearing material for total joint arthroplasty such as for the hip, knee, and shoulder for several decades, whereas spine applications have drawn increasing interest especially in the last few years, see Kurtz.[1] Here, total joint arthroplasty stands for a replacement of both articulating surfaces of the diseased joint to be surgically reconstructed.[2] The most important application for medical UHMWPE is the use as one component in the metal-on-UHMWPE implant, contrary to metal-on-metal or ceramic-on-ceramic total joint replacements.

The extremely high molar mass of UHMWPE provides a large potential for chain folding and entanglements, which is essential for outstanding tribological properties, see Goldman et al.[3] Nevertheless, the wear of conventional UHMWPE is still a problem of highly stressed bearings as hip and knee replacements. Therefore, highly crosslinked polyethylenes have been developed that may reduce the wear substantially, see Becker et al.[4] On the other hand, it is known that crosslinking reduces the mechanical properties, as strain to failure and crack resistance.

For medical applications, the electron or gamma beam irradiation[3,5,6] is widely used to prepare chemically crosslinked structures. With respect to the required high purity for medical applications, crosslinking via modified chemical reactions such as suitable reactants or additives is not applicable.[1] In the case of irradiation, a high ionizing radiation energy is chosen to initiate scissions of C—C and C—H bonds leading to a large number of alkyl radicals.[1] Those are needed to form a chemically crosslinked 3D structure of covalent bonds between adjacent chain molecules. However, the free radicals are very mobile and can also lead to recombination processes. Goldman et al.[3] reported about a long lifetime of many months for the free radicals. Especially, the oxygen with its high diffusion mobility is very active with the radicals, which may enable oxidative degradation.

The linear polyethylene with its monomeric unit —[CH_2—CH_2]— can easily crystallize to achieve a maximum degree of crystallinity of 60–80% for the short-chain branched (2 CH_3/1000 C atoms) HDPE and 40–65% for the long-chain branched (10–35 CH_3/1000 C) LDPE with an average molar mass in technical applications of about 1 and 0.2–0.5 $\times$ 10^5 g/mol, respectively. In comparison, the UHMWPE

Correspondence to: U. Göschel (ulrich.goeschel@ikt.uni-stuttgart.de).

with its extraordinary large chain length (molar mass: 2–6 $\times$ 10^6 g/mol) and high entanglement density may result in a maximum degree of crystallinity of up to 60%, which is somewhat lower than that for the commercial HDPE.

Polyethylene is known for its three kinds of relaxation processes in the entire temperature range as is seen in dynamic mechanical thermal (DMTA),[7–14] dielectric,[15,16] and nuclear magnetic (NMR) experiments,[10,14,17] With respect to, e.g., Zamfirova et al.,[8] UHMWPE exhibits the γ, β, and α relaxations, characterized by a loss modulus (E'') maximum at -113 to -111°C, -4°C, and 57–58°C, respectively, as determined from tensile DMTA measurements at an angular frequency ($\omega = 2\pi f$) of 18.8 Hz.

The γ relaxation is considered as the glass transition temperature for unbranched polyethylene; see Stehling and Mandelkern.[9] Those authors have shown that the intensity of the γ relaxation increases as crystallinity decreases. Kawai et al.[18] have discussed the β relaxation as assigned to interlamellar grain boundary phenomena associated with orientational and distortional dispersions of noncrystalline materials between oriented lamellae. The α relaxation has been addressed to chain mobility in crystallites as derived by Hu and Schmidt-Rohr[17] from NMR studies. Kawai et al.[18] distinguish between the α_1 and α_2 relaxation associated with intralamellar grain boundary phenomena and intracrystal lattice retardation phenomena, respectively.

This article will gain new insights into the mechanical relaxation of medical grade UHMWPE of different crosslink density as prepared by electron beam irradiation on preexisted crystalline structures. The question arises in which way crosslinking can proceed. Here, effects of the irradiation on the crystalline structure as well as effects of the crystalline structure on the crosslinking have to be considered. The phenomena crosslinking and crystallization can take place simultaneously and will influence each other. Studies on the chain mobility as characterized by DMTA will be chosen as a sensitive discriminator for contributions from chain architecture in both the crystalline entities and crosslinked phases.

EXPERIMENTAL

Materials

UHMWPE medical grade resin GUR 1050 from Ticona GmbH, Oberhausen with a molar mass of 6 $\times$ 10^6 g/mol (free of calcium stearate additives) was compression molded into plates by Quadrant Engineering Plastic Products, Vreden. Those plates were cut into bars of 30 $\times$ 65 $\times$ 500 mm^3 for a warm-irradiation by means of adiabatic melting (WIAM) processes performed by Zimmer GmbH, Winterthur, Switzerland.[19] Using a 10-MeV Rhodotron electron beam accelerator, the materials were heated to 120°C and exposed to 0, 50, 95, and 110 kGy as denoted with WIAM 0, WIAM 50, WIAM 95, WIAM 110, respectively. Thereafter, the materials were annealed at 150°C for 5 h and subsequently slowly cooled to room temperature to eradicate the free radicals. Because of the oxygen in the air, the surface layer was oxidized and therefore omitted in the experiments.

Methods

Trans-vinylene index

The treatment with ionizing radiation leads to *trans*-vinylene unsaturations by abstracting a hydrogen molecule from the polymer chain. The amount of those unsaturations increases with the applied radiation dose. Therefore, the *trans*-vinylene index (TVI) can be used as an internal dosimeter.

Applying FTIR spectroscopy, the TVI was determined from the peak area for the *trans*-vinylene vibration at 965 cm^{-1} normalized to the peak at 1370 cm^{-1} according to the standard ASTM F 2381-04.[20] The FTIR spectra were collected in transmission mode using a Bruker Equinox 55 spectrometer combined with a FTIR microscope Bruker IR-Scope I with a resolution of 4 cm^{-1}. Thin films with a thickness of about 0.2 mm were prepared out of the delivered bars by applying an engine lathe of a low rotational speed of 150 U/min (Fig. 1). Only nonoxidized material was used as taken 5 mm below the surface layer. The TVI values are the average from four single measurements.

Crosslink density

Equilibrium swelling experiments were performed in *o*-xylene with 0.2 mass % Irganox 1010 (Ciba Geigy) added as an antioxidant. The samples were kept at 130°C for 24 h and then weighed. After cooling to room temperature in the extractor hood, the specimens were dried in a vacuum oven at 60°C to reach a constant weight. The swell ratio (q) was calculated from the weight ratio between the swollen and the dried extracted gel according to the standard ASTM F 2214-02[21] and Shen et al.[7] The values stated below are the average of three tests.

With the steady-state swell ratio (q), the crosslink density (ν_d) was computed using Flory's network theory[22] expressed by eq. (1).

$$\nu_d = -\frac{\ln(1-q^{-1}) + q^{-1} + \chi_F q^{-2}}{V_1(q^{-1/3} - 0.5q^{-1})} \quad (1)$$

Flory's interaction parameter for *o*-xylene–PE at 130°C with $\chi_F = 0.33 + 0.55/q$,[21] the molar volume of *o*-xylene $V_1 = 136$ cm^3/mol and the eq. (2) were

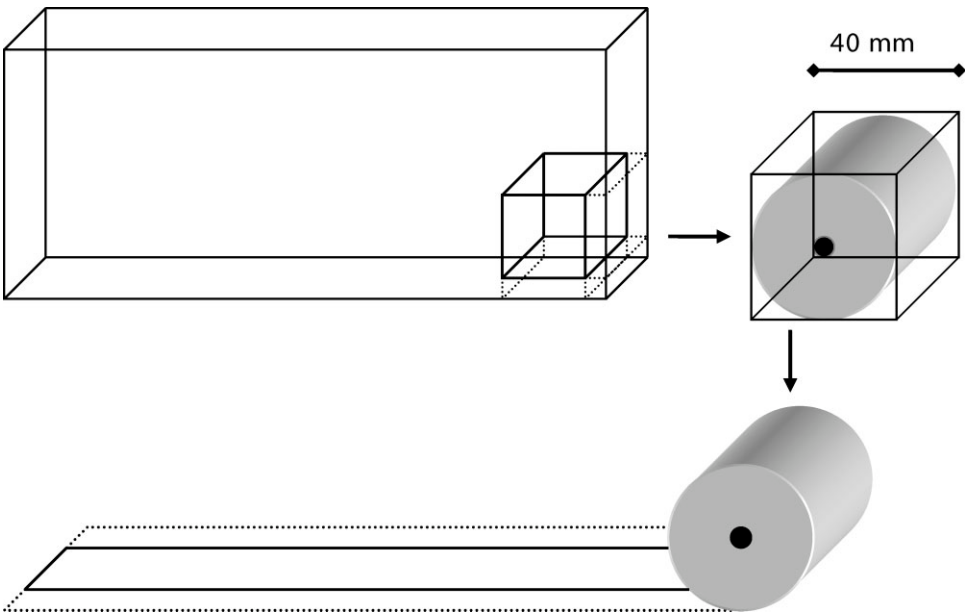

Figure 1 Sampling to assemble the films, the cylinder was transferred to a lathe to preturn the film.

applied to calculate the molar mass between adjacent crosslinks (M_c),

$$M_c = \frac{\rho_{\text{solid}}}{\nu_d} \tag{2}$$

Here, a density of $\rho_{\text{solid}} = 0.92$ g/cm^3 was used.

Transmission electron microscopy

The samples for transmission electron microscopy (TEM) experiments were prepared by staining with RuO_4 vapor at 23°C for 16 h,[23] subsequently rinsed in distilled water, dried, embedded in epoxy resin, and cured at 23°C over night. Thereafter, thin slices of 80–100 nm were sectioned at 23°C by the ultramicrotome Reicher-Jung, Ultracut E, FC 4D using a diamond knife. The TEM studies were performed at a Zeiss EM-10 at 100 kV.

Differential scanning calorimetry

Differential scanning calorimetry (DSC) experiments were carried out using a Mettler DSC821e/700 under nitrogen atmosphere. The temperature scale was calibrated by the use of *n*-heptane (90.5°C), water (0.0°C), indium (156.6°C and heat capacity), lead (327.5°C), and zinc (419.5°C and heat capacity). Each sample of about 10 mg was heated from −50 to +200°C (first heating run), cooled to −50°C, and heated again to +200°C (second heating run). Heating and cooling rates of 10 K/min were chosen. Thus, the melting (T_m) and crystallization temperature (T_c), onset crystallization temperature ($T_{c,\ \text{onset}}$), enthalpy of melting (ΔH_m), and crystallization (ΔH_c) were determined. The degree of crystallinity (χ) was calculated from the experimental melting enthalpy (ΔH_m) using eq. (3) and the melting enthalpy of 100% crystalline UHMWPE with $\Delta H_m^c = 291$ J/g.[24]

$$\chi = 100\% \Delta H_m / \Delta H_m^c \tag{3}$$

With respect to Hoffman et al.,[25] the average thickness of the crystallites (d_c) was obtained from the experimental melting peak absolute temperature (T_m) using the Gibbs–Thompson eq. (4), which describes the melting point depression originated by the finite size of the crystallites in one direction, see Strobl.[26]

$$d_c = \frac{2\sigma_e}{\Delta h_f}\left(1 - \frac{T_m}{T_m^o}\right)^{-1} \tag{4}$$

Here, $T_m^o = 418.95$ K is the extrapolated equilibrium melting temperature of a PE crystal of infinite thickness, $\sigma_e = 9.3 \times 10^{-2}$ J m^{-2} is the lamellar basal surface free energy, and $\Delta h_f = 2.80 \times 10^8$ J m^{-3} is the heat fusion per unit volume.[27]

Mechanical tensile testing

Stress–strain experiments were performed by a Zwick 1476 universal tensile testing machine applying DIN EN ISO 527-2. Specimens of 4.0 × 0.2 mm^2 (width × thickness) were chosen in accordance to the geometry S3A in DIN 53504. The traverse speed was set to 20 mm/min at a sample length $L_0 = 10$ mm. A small preload of 0.1 MPa was used. The elastic modulus was determined in the strain range $0.5\% \leq \varepsilon \leq 0.7\%$, where elastic deformation behavior exists. With respect to DIN EN ISO 291-23/50-2, the samples were stored for 24 h at least in standard climate (23°C, 50% relative humidity) before testing. Five samples were run for each material tested.

Dynamic mechanical thermal analysis

A relaxation spectrometer Rheometrics RMS-800 RDS II at a sinusoidal oscillatory shear deformation $\gamma(t)$ was used, see eq. (5).

$$\gamma(t) = \gamma_0 \sin(\omega t) \tag{5}$$

The dynamic measurements were subjected to a small strain amplitude of $\gamma_0 = 0.2\%$ at a sample length of $L_0 = 30$ mm (distance between the clamps) and a small static loading of 1.2 MPa at a sample geometry of $4 \times 10 \times 34$ mm^3 (thickness × width × length) to ensure linear viscoelastic behavior. The experiments were performed at different angular frequencies ($\omega = 2\pi f$) in a logarithmic scale of 0.6, 1.4, 2.9, 6.3, 13.5, 29.2, 63.8, and 135.4 Hz during a stepwise increase of the temperature by 5 K, at a rate of 5.0 K/min subsequent to a holding time of 3 min. The resulting sinusoidal stress response $\sigma(t)$ was shifted by the phase angle (δ) against the shear deformation. Recorded are the output in terms of the temperature dependence of the complex shear modulus (G^*), storage modulus (G'), shear loss modulus (G''), and loss tangent (tan δ) in the range from −150 to +140°C as a function of the angular frequency (ω), eqs. (6) and (7).

$$\frac{\sigma(t)}{\gamma_0} = G^* = G'(\omega)\sin(\omega t) + G''(\omega)\cos(\omega t) \tag{6}$$

$$\tan\ \delta = \frac{G''(\omega)}{G'(\omega)} \tag{7}$$

With respect to the frequency-temperature-correlation principle, an increase in the temperature will shift the G'' dispersion to higher frequencies. That was used to determine the activation energy (ΔE_a) of each relaxation mode from the frequency (f) dependence of the mechanical loss modulus (G'') maximum with the universal gas constant $R = 8.314$ J/(mol K) and the absolute temperature (T) according to the Arrhenius law in eq. (8)

$$f(T) = f_0 \exp\left(-\frac{\Delta E_a}{RT}\right) \tag{8}$$

where the slope in the graph

$$\ln f_{G'' \max} = \frac{-\Delta E_a}{R}\ \frac{1}{T} \tag{9}$$

was used to determine the activation energy (ΔE_a) in the unit kJ/mol.

RESULTS AND DISCUSSION

Trans-vinylene index

The TVI relates to the number of abstracted hydrogen molecules due to electron beam irradiation. It has been shown that the TVI increases almost arithmetically from 0.026 to 0.057 with the increase in the irradiation dose from 50 to 110 kGy (Fig. 2), which proves the increasing effect of the irradiation dose on the molecular structure. Experiments on different sample positions reveal only minor variations in TVI by about 3%. That is a result of a uniform irradiation dose distribution over the whole sample.

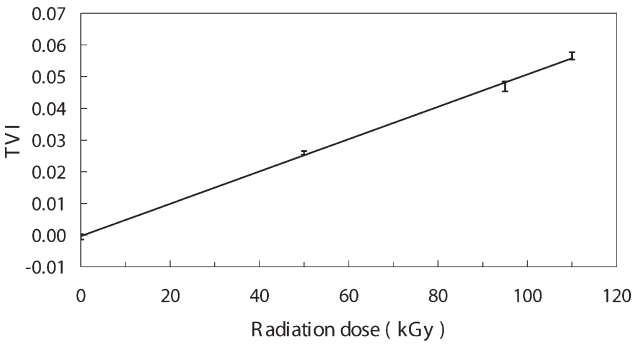

Figure 2 *Trans*-vinylene index (TVI) of UHMWPE of different irradiation dose.

Crosslink density

From equilibrium swelling experiments at 130°C in *o*-xylene applying a swelling time of 24 h, the crosslink density (ν_d) and the molar mass between adjacent crosslinks (M_c) have been calculated from the swell ratio (q) using the eqs. (1) and (2). Preliminary swelling studies documented that the equilibrium for the irradiated WIAM 50, WIAM 95, and WIAM 110 could be reached in less than 10 h. However, in the case of the nonirradiated WIAM 0, the equilibrium was approached without reaching it even at very long times of 50 h. The steady dissolving process leads to a continuous decrease in the remaining nondissolved sample, which results in an increase in the q-value, see eq. (1). That prevents a reliable determination of the crosslink density of the nonirradiated material.

The irradiation at 50 kGy led to a molar mass between adjacent crosslinks of 4270 g/mol. An increase in the irradiation dose to 110 kGy caused a further reduction to 3170 g/mol, which corresponds to 113 monomeric units (Table I).

Transmission electron microscopy

The TEM images on the WIAM samples reveal a lamellar structure of two different lateral dimensions. The white lines in Figure 3 correspond to the crystallites arranged in lamellae layers, which are separated by amorphous regions. The latter appear in black color because of the high absorption of the electron beam in the RuO_4-rich disordered phases

TABLE I
Swell Ratio (q), Crosslink Density (υ_d), and Molecular Mass between Adjacent Crosslinks (M_c) of the Irradiated UHMWPE

Sample	Swell ratio, q	Crosslink density, υ_d (mol/dm^3)	Molar mass between adjacent crosslinks, M_c (g/mol)	Number of monomeric units between adjacent crosslinks
WIAM 50	2.97 ± 0.01	0.216 ± 0.001	4,270 ± 15	152
WIAM 95	2.60 ± 0.01	0.286 ± 0.003	3,220 ± 37	115
WIAM 110	2.58 ± 0.02	0.290 ± 0.004	3,170 ± 47	113

subsequent to the staining process. The thinner lamellae exhibit a thickness of about 7.5–10 nm for the nonirradiated WIAM 0 (Fig. 3, left) and about 5 nm for the irradiated WIAM 95 (Fig. 3, right) and WIAM 110. Those lamellae are oriented. Additionally, all WIAM samples show larger lamellae with a thickness of about 20 nm, which are randomly oriented. Finally, the irradiation leads to a decrease in the thickness of the smaller lamellae, whereas the larger lamellae remain unchanged.

In comparison, Farrar and Brain[28] discussed the existence of lamellae in extruded GUR 415 and nonirradiated UHMWPE with a thickness of $\sim$ 15–20 nm from TEM images. Kurtz et al.[2] reported about crystalline lamella with a thickness of 10–50 nm. Those lamellae are planar entities and consist of molecular chains that are perpendicular to the plane and fold back and forth. By means of TEM and SAXS experiments, Goldman et al.[3] determined a lamellar thickness in the order of 50 nm developed for gamma as well as electron beam-irradiated (GUR 1020) UHMWPE, both at an irradiation dose of about 25 kGy. Additionally, those authors[3] have shown that the SAXS long period (L), which is equal to the sum of crystalline and amorphous regions (ideal two-phase structure), remains unchanged in the time range from 1 to 11 months. Here, the long period $L = 2\pi/q$ was obtained from the peak position in the scattering intensity curve $I = f(q)$ using the scattering vector $q = 4\pi \sin \theta/\lambda$, where λ is the X-ray wavelength and 2θ is the scattering angle. Only the scattering intensity (I) decreases with time leading to the assumption that either fewer crystalline/amorphous boundaries are present or those boundaries are less sharp. Nevoralová et al.[29] reported on UHMWPE about a decrease of the SAXS long period from 37.5 to 32.5 nm with an increase of the gamma irradiation dose from 0 to 200 kGy applying a dose rate of 0.25 kGy/h. In contrast, a higher dose rate of 2.5 kGy/h has shown a minimum of 32.5 nm at 100 kGy followed by a slight increase to reach 33 nm at 200 kGy. It was supposed that chain scission upon irradiation as occurred mainly in the amorphous phase leads to the formation of additional and thinner lamellae in those regions.

Differential scanning calorimetry

The DSC experiments were performed by a heating, subsequent cooling, and second heating run. The latter is free of any effects because of mechanical and thermal loading during processing and reveals an endothermic melting temperature of 136.8 and 140.9°C for the nonirradiated and the 110 kGy-irradiated sample, respectively, (Table II). The degree of crystallinity (χ) as determined from the melting enthalpy in the second heating run and using eq. (3)

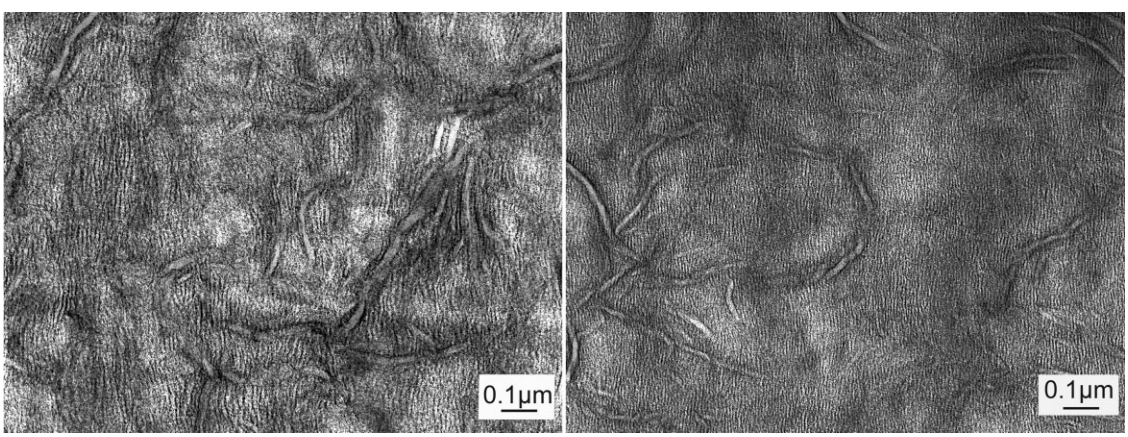

Figure 3 TEM image on ultra-thin UHMWPE slices of different irradiation dose with 0 (left) and 95 kGy (right). The magnification is ×50,000.

TABLE II
DSC Characteristics of UHMWPE of Different Irradiation Dose during the Second Run of Melting

Sample	Melting peak temperature, T_m (°C)	Average thickness of crystallites, d_c (nm)	Enthalpy of melting, ΔH_m (J/g)	Degree of crystallinity, χ (%)
WIAM 0	136.8 ± 0.4	30.9	152.0 ± 0.6	52.2
WIAM 50	138.0 ± 0.2	35.7	148.2 ± 0.2	51.0
WIAM 95	141.6 ± 0,4	66.3	145.9 ± 2.0	50.1
WIAM 110	140.9 ± 1.2	56.8	144.4 ± 14.9	49.6

decreases slightly from 52.2 to 49.6% with increasing irradiation dose (Table II). The melting enthalpy at the highest irradiation dose of 110 kGy shows an extraordinary large standard deviation. Stephens et al.[30] discussed a slight increase followed by a decrease in the degree of crystallinity from DSC data with an increase in the gamma irradiation dose (75 and 150 kGy) and dose rate (0.25 and 2.9 kGy/h) of UHMWPE. They suggested that the decrease in crystallinity is related to an increase in the crosslink density, whereas a chain scission should lead to an increase in the crystallinity.[31]

The melting peak of the second heating run (Fig. 4) shows the formation of a shoulder at 128°C for 50 kGy. With increasing beam doses, the shoulder turns into a well-established additional melting peak at the low-temperature side at about 120°C for both 95 and 110 kGy (Fig. 4). The origin of those low-temperature peaks can be related to the existence of lamellae with a variation in thickness and crystalline order. Stephens et al.[30] also reported about two existing DSC and SAXS peak values, which are originated by two different crystal dimensions.

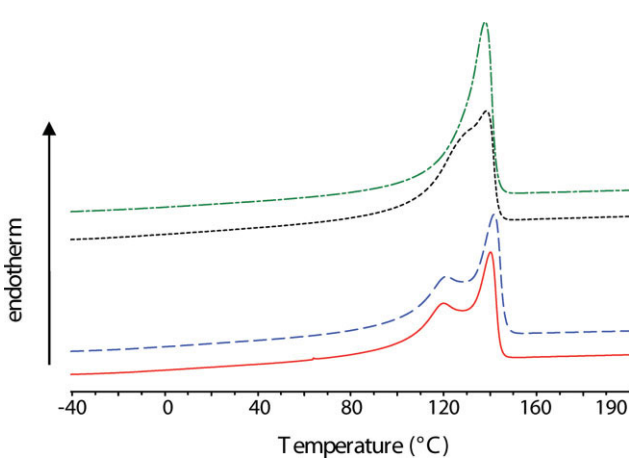

Figure 4 DSC traces of UHMWPE of different irradiation dose with 0 kGy (– · –), 50 kGy (- - -), 95 kGy (– –), and 110 kGy (—) during endothermic melting in the second heating run. [Color figure can be viewed in the online issue, which is available at www.interscience.wiley.com.]

The Gibbs–Thompson eq. (4) was used to calculate the average lamellae thickness from the experimental melting peak temperatures. With respect to the melting temperatures at the high-temperature side in Figure 4 during the second heating run, the lamellae thickness strongly increases from 30.9 to 66.3 nm with an increase in the irradiation dose from 0 to 95 kGy (Table II). A further increase in the beam dose from 95 to 110 kGy results in a slight decrease in the lamellae thickness. Such a tendency is in agreement with gamma irradiation experiments of Stephens et al.[30] Bartczak and Lezak[32] discussed about a lamellae thickness of 17.4 nm obtained from DSC using the Gibbs–Thompson eq. (4) and a long period of 33.3 nm from SAXS for UHMWPE from Ticona with $M_w = 5.5 \times 10^6$ g/mol, which is almost comparable to the nonirradiated WIAM 0. In comparison, Cook et al.[27] reported about DSC studies applying the Gibbs–Thompson eq. (4) on nascent powder and ram-extruded but nonirradiated (GUR 415) UHMWPE with a molar mass of 6×10^6 g/mol with a crystalline lamellae of 58 ± 13 and 28 ± 4 nm, respectively.

From the low-temperature peak, thin lamellae of 20.2 (at 50 kGy) and 10.8 nm (at 95 and 110 kGy) are detected by applying the Gibbs–Thompson eq. (4). Such a phenomenon was also discussed by Nevoralová et al.[29]

The crystallization peak as obtained during cooling subsequent to the first melting is characterized by an exothermic peak and the formation of an additional peak at the low-temperature side at about 106°C (Fig. 5). As determined from the main peak, the crystallization peak and thus the onset of crystallization shift toward higher temperatures from 113.4 to 125.1°C and from 121.2 to 130.8°C, respectively, with increasing irradiation dose (Table III). Such an increase is equal to a rise in the crystallization rate as probably originated by mobile chain fractions because of irradiation. Isothermal and nonisothermal synchrotron WAXD experiments[33] confirm the acceleration in crystallization as seen by DSC. Furthermore, an increase in the irradiation dose leads to a decrease in the crystallization enthalpy (equal to a

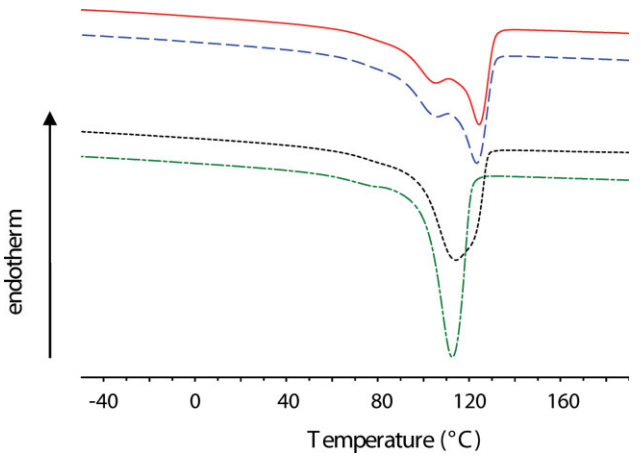

Figure 5 DSC traces of UHMWPE of different irradiation dose with 0 kGy (– · –), 50 kGy (---), 95 kGy (– –), and 110 kGy (—) during exothermic crystallization subsequent to cooling from the first melting. [Color figure can be viewed in the online issue, which is available at www.interscience.wiley.com.]

decrease in the degree of crystallinity) from 150.1 to 143.1 J/g.

Mechanical tensile testing

Applying an averaged strain rate of about 67%/min, the elastic modulus (E), yield stress (σ_y), and strain at break (ε_{Br}) decrease significantly with the irradiation dose, except the elastic modulus (E) for WIAM 50 (Fig. 6, Table IV). The elastic modulus characterizes the material stiffness, which is highest for the nonirradiated WIAM 0 with 697 MPa in comparison to 560–591 MPa for the irradiated UHMWPE. Furthermore, WIAM 0 reveals the highest strain at break with $\varepsilon_{Br} > 455\%$ (without reaching the break), and the lowest plastic deformation as documented by the largest yield stress of 19.9 MPa and the highest stress values at comparable strain above the yielding. It is known that the yield stress usually increases with an increase in the degree of crystallinity, crystal thickness, and crosslink density. Chosen a strain ($\varepsilon_{200\%}$) at 200% out of the plastic deformation region, the corresponding stress ($\sigma_{200\%}$)

TABLE III
DSC Crystallization Characteristics of UHMWPE of Different Irradiation Dose during the Cooling Run Subsequent to the First Melting

Sample	Crystallization peak temperature, T_c (°C)	Onset crystallization temperature, $T_{c,\,onset}$ (°C)	Enthalpy of crystallization, ΔH_c (J/g)
WIAM 0	113.4 ± 0.5	121.2 ± 0.3	150.0 ± 0.7
WIAM 50	114.2 ± 0.3	128.4 ± 0.3	147.4 ± 0.2
WIAM 95	123.1± 0.5	130.8 ± 0.4	145.1 ± 1.9
WIAM 110	125.1 ± 2.9	130.8 ± 0.8	143.1 ± 15.2

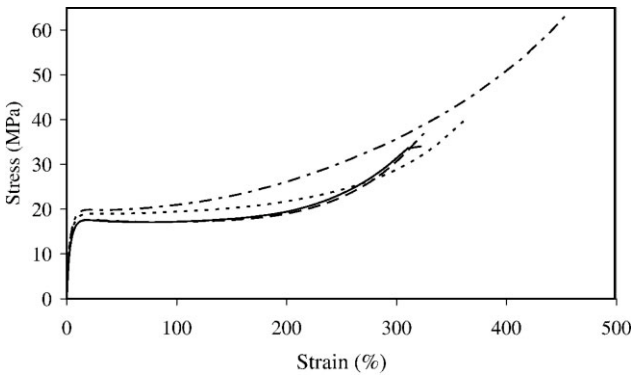

Figure 6 Mechanical stress–strain curve of UHMWPE of different irradiation dose with 0 kGy (– · –), 50 kGy (---), 95 kGy (– –), and 110 kGy (—).

decreases significantly with the irradiation dose (Table IV). At deformations above the yielding, chain slip processes in the crystalline phase (e.g., among certain crystallographic planes) as well as in the amorphous phases (e.g., interlamellar sliding and interlamellar separation) have to be considered, see, e.g., Bartczak and Lezak.[32] Those deformation mechanisms result in significant morphological and property changes. The tendency of a loss in the mechanical properties with irradiation dose has already been reported for gamma[34] as well for electron beam-irradiated UHMWPE.[19]

Dynamic mechanical thermal analysis

The DMTA results will be discussed in terms of the temperature dependency of the storage shear modulus (G') and the loss shear modulus (G'') in the range from −150 to +140°C at different angular frequencies ($\omega = 2\pi f$) from 0.6 to 135.4 Hz, which are related to the material stiffness and the molecular mobility, respectively.

From the temperature-dependent loss shear modulus (G''), three different relaxation processes can be distinguished (Figs. 7 and 8). For those γ, β, and α relaxations, a peak maximum ($T_{G''max}$) in G'' at −118 to −121°C, −26°C, and 47 to 56°C, respectively, has been determined for an angular frequency (ω) of 6.3 Hz (Table V). An increase in the frequency (ω) from 0.6 to 135.4 Hz leads to a significant shift of the relaxation peaks toward higher temperatures (Fig. 8), which has been used to determine the activation energy (ΔE_a) by means of eq. (9). According to Stehling and Mandelkern,[9] the γ relaxation relates to the glass transition. The corresponding activation energy (ΔE_a) for all WIAM materials varies only in the small range from 84 to 86 kJ/mol (Table V). For PE films and fibers of low molar mass, characterized by a viscosity-average molar mass of $M_v \leq 70{,}000$, Matsuo et al.[10] have found that the temperature peak of the

TABLE IV
Mechanical Data of UHMWPE of Different Irradiation Dose as Obtained from Tensile Experiments at Room Temperature

Sample	Elastic modulus, E (MPa)	Yield stress, σ_y (MPa)	Yield strain, ε_y (%)	Stress at $\varepsilon = 200\%$, σ_{200} (MPa)	Stress at break, σ_{Br} (MPa)	Strain at break, ε_{Br} (%)
WIAM 0	697 ± 39	19.9 ± 0.5	22.0 ± 2.4	26.1 ± 0.7	>63.5[a]	>455[a]
WIAM 50	560 ± 19	19.0 ± 0.3	23.9 ± 3.1	21.7 ± 0.2	40.5 ± 4.4	365 ± 19
WIAM 95	591 ± 39	17.7 ± 0.7	20.4 ± 1.8	19.0 ± 0.7	37.0 ± 0.9	325 ± 7
WIAM 110	567 ± 41	16.5 ± 0.8	18.1 ± 1.2	17.2 ± 0.8	34.0 ± 1.9	322 ± 10

[a] No break.

γ relaxation is independent of the molecular orientation and crystallinity. Zamfirova et al.[8] reported about an activation energy (ΔE_a) of 106–107 kJ/mol for UHMWPE of different cocatalyst systems.

The β relaxation is rather weak (Figs. 7 and 8) and consequently, it is difficult to determine the corresponding activation energy (ΔE_a). The weakness of the β relaxation has already been reported by other authors, e.g., Hronský et al.[14] and Zamfirova et al.[8] Only in the case of the nonirradiated WIAM 0, the frequency shift in the G'' modulus provides a trustful value for ΔE_a, which is 116 kJ/mol (Table V). With respect to Kawai et al.,[18] the β relaxation arises from interlamellar grain boundary phenomena associated with orientational and distortional dispersions of noncrystalline materials between oriented lamellae. Further structural insights are needed to explore that phenomenon for the WIAM materials.

Major changes are seen for the α relaxation (Figs. 7 and 8). Here, the activation energy (ΔE_a) decreases from 136 (WIAM 0) to 108 kJ/mol (WIAM 110) with increasing irradiation dose (Table V). Additionally, the peak temperature ($T_{G''\max}$) at $\omega = 6.3$ Hz is different for the nonirradiated WIAM 0 with 56°C in comparison to the irradiated WIAM 50, 95, and 110 with 48 or 47°C (Table V). Yeh et al.[12] discussed the effects that the restrained chain mobility, resulted from extraordinary long UHMWPE molecules in the crystal and interfacial regions, are much higher than those from low chain molecules. That is why, a much higher temperature is required to motivate the molecular motions of UHMWPE resulted from the α transition. According to Hu and Schmidt-Rohr,[17] the activation energy of the α relaxation is addressed to chain mobility in crystallites. Kawai et al.[18] have discussed the existence of an α_1 and α_2 relaxation

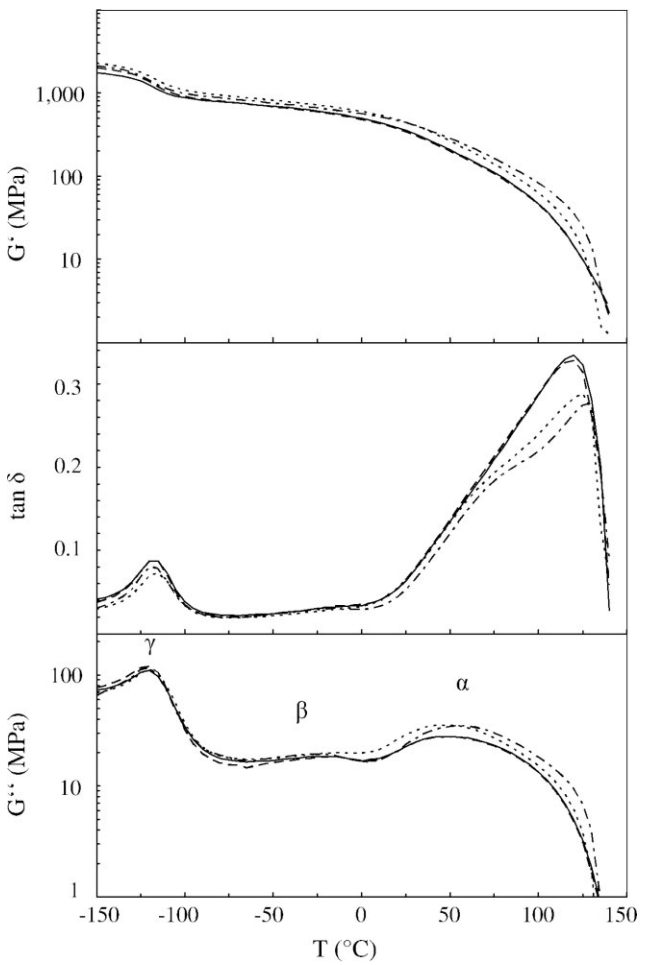

Figure 7 Temperature dependence of the storage shear modulus (G'), the loss tangent (tan δ), and the loss shear modulus (G'') of UHMWPE of different irradiation dose with 0 kGy (– · –), 50 kGy (---), 95 kGy (– –), and 110 kGy (—) as determined at an angular frequency ($\omega = 2\pi f$) of 6.3 Hz.

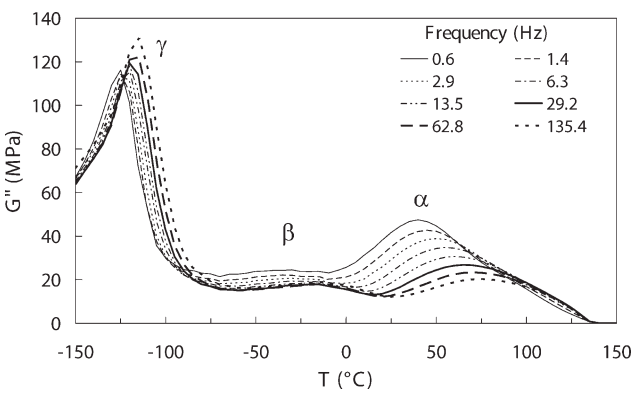

Figure 8 Temperature dependence of the loss shear modulus (G'') of the nonirradiated UHMWPE at frequencies ($\omega = 2\pi f$) of 0.6, 1.4, 2.9, 6.3, 13.5, 29.2, 62.8, and 135.4 Hz.

TABLE V
Peak Temperature ($T_{G''max}$) and Activation Energy (ΔE_a) of the γ, beta, and α Relaxation of UHMWPE of Different Irradiation Dose

	γ Relaxation		β Relaxation		α Relaxation	
	$T_{G''max}$ (°C)	ΔE_a (kJ/mol)	$T_{G''max}$ (°C)	ΔE_a (kJ/mol)	$T_{G''max}$ (°C)	ΔE_a (kJ/mol)
WIAM 0	−121	85	−26	116	56	136
WIAM 50	−118	84	–	–	48	126
WIAM 95	−121	86	–	–	48	112
WIAM 110	−120	85	–	–	47	108

$T_{G''max}$ was obtained from the peak of the G'' modulus at an angular frequency ($\omega = 2\pi f$) of 6.3 Hz.

related to intralamellar grain boundary phenomena and intracrystal lattice retardation phenomena, respectively. Figure 7 shows a well-established α relaxation, however, no split into α_1 and α_2.

The storage shear modulus (G') at an angular frequency (ω) of 6.3 Hz decreases with a temperature increase from −150 to about +140°C (Fig. 7). At temperatures below the glass transition temperature (γ relaxation in Fig. 7), the G' modulus is nearly temperature independent, which represents the almost nonrelaxed state. Consequently, the material stiffness (G' modulus) from that region should increase with an increase in the crystal order and crosslink density and with a decrease in the number of chain scissions. The G' modulus of WIAM 0, 95, and 110 at −140°C decreases with an increase in the irradiation dose. That tendency is in agreement with the elastic tensile modulus (E) of the materials above room temperature, see Figure 6 and Table IV. However, the crystallinity from DSC (Table II) and the crosslink density from swelling experiments (Table I) cannot explain the loss in material stiffness with increasing irradiation dose. Probably, there are effects in relation to the fine crystal order and changes in the molar mass distribution due to chain scissions, which have to be considered. Differences in the crystal order are seen by TEM (Fig. 3), which documents the existence of lamellae of two different sizes, where the smaller one decreases in the thickness with irradiation. The comparison between WIAM 0 and WIAM 50 shows the higher G' modulus at −140°C for the WIAM 50 (Table VI), which is in agreement to the increase in the crosslink density due to irradiation (Table I) and does not corolate with the elastic tensile modulus (E) in Figure 6 and Table IV.

The chain mobility of the existing morphology will be discussed by means of the relaxation strength ($\Delta G'_\gamma$) in the glass transition region and its relative value ($\Delta G'_{\gamma,rel}$) as determined from the difference in G' at −140 and −70°C using eqs. (10) and (11), respectively.

$$\Delta G'_\gamma = G'(-140°C) - G'(-70°C) \quad (10)$$

$$\Delta G'_\gamma, \text{rel} = 100\% \Delta G'_\gamma / G'(-140°C) \quad (11)$$

Here, the chosen temperatures represent the lower and upper temperature limits of the γ relaxation (Fig. 7). As is known, a decrease in both the crystal order and crosslink density and an increase in the number of chain scissions will enhance the chain mobility. The relative relaxation strength ($\Delta G'_{\gamma,rel}$) is the lowest for the WIAM 110 (Table VI). Probably, this is related to effects of chain scissions due to the high irradiation dose.

The material stiffness (G') at high temperatures close the melting can be enhanced by an increase in the crystal order and crosslink density. Out of this temperature range, the G' modulus at +125°C and an angular frequency (ω) of 6.3 Hz were chosen for discussion (Table VI). To some surprise, the G'

TABLE VI
DMTA Storage Shear Modulus (G') at Different Temperatures and Relaxation Strength ($\Delta G'_\gamma$) in the Glass Transition of UHMWPE of Different Irradiation Dose as Determined at an Angular Frequency ($\omega = 2\pi f$) of 6.3 Hz

	Storage shear modulus at				Relaxation strength[a]	Relative relaxation strength[a]
Sample	−140°C, G' (MPa)	−70°C, G' (MPa)	+25°C, G' (MPa)	+125°C, G' (MPa)	$\Delta G'_\gamma$ (MPa)	$\Delta G'_{\gamma,rel}$ (%)
WIAM 0	2,000	836	442	25	1,164	58.2
WIAM 50	2,140	903	447	13	1,237	57.8
WIAM 95	1,890	757	343	10	1,133	59.9
WIAM 110	1,650	756	355	10	894	54.1

[a] Using the storage shear modulus (G') at −140 and −70°C and eq. (10) or (11).

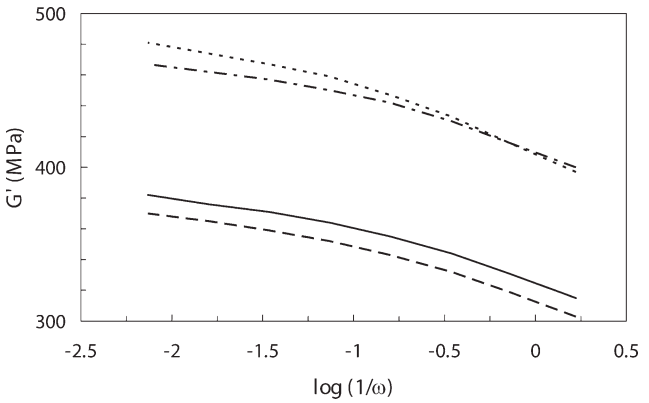

Figure 9 Frequency dependence of the storage shear modulus (G') of UHMWPE of different irradiation dose with 0 kGy (– · –), 50 kGy (---), 95 kGy (– –), and 110 kGy (—) as determined at a temperature of 25°C.

(125°C) modulus is higher for the nonirradiated WIAM 0 than for the irradiated WIAM 50, 95, and 110. Moreover, an irradiation dose of 50 kGy (WIAM 50) leads to a higher G' (125°C) than that of 95 (WIAM 95) and 110 kGy (WIAM 110). However, additional information on molecular ordering and molar mass distribution is required to explain that uncertain behavior at high temperatures.

Figure 9 represents a decrease in the storage shear modulus (G') with an increase in the reciprocal angular frequency ($1/\omega$) at a chosen temperature of 25°C. This corresponds to a decrease in the material stiffness with time originated by the relaxation behavior of mobile chain segments in the amorphous phase. The slope of the curves is almost identical for WIAM 0, 50, 95, and 110, whereas the G' modulus is similar for WIAM 0 and 50 as well as for WIAM 95 and 110.

Usually, crosslinking is expected to lead to a higher material stiffness. However, the crosslink density as determined by swelling experiments does not characterize the entanglement density, which is "effective" under mechanical loading. That is mainly due to the different time constant between equilibrium swelling and mechanical experiments. To achieve a structure of disentangled chains during swelling, a high temperature of 130°C and a long dissolving time of 24 h were applied. Therefore, the resulting crosslink density obtained from equilibrium swelling is much higher than that, which is "effective" in short-term mechanical tensile testing at a strain rate of 67%/min or DMTA at the angular frequencies (ω) ranging from 0.6 to 135.4 Hz.

CONCLUSIONS

In this article, the effect of electron beam irradiation on crystallized medical grade UHMWPE has been studied. In the focus are the formation of a chemically crosslinked structure as characterized by a significant decrease in the molar mass between adjacent crosslinks to reach 3170 g/mol at lowest. The crosslinking proceeds with almost no change in the degree of crystallinity of about 50%, whereas the lamellae thickness changes and new thin lamellae grow. DMTA in the angular frequency range from 0.6 to 135.4 Hz has been employed to discriminate between effects from crosslinking and crystallization. Discussed is the molecular mobility of three relaxations of different temperature position and activation energy with respect to morphological changes upon irradiation. Here, the high temperature α relaxation from 47 to 56°C at $\omega = 6.3$ Hz is shown to be very sensitive to irradiation. Further studies are needed to explore the mechanism of crosslinking under the consideration of significant changes in the crystalline structure.

The authors thank N. A. Abt, Zimmer GmbH, Winterthur, Switzerland for providing the electron beam-irradiated UHMWPE materials and his helpful discussions.

References

1. Kurtz, S. M. The UHMWPE Handbook: Ultra-High Molecular Weight Polyethylene in Total Joint Replacement; Elsevier Academic Press: Amsterdam, 2004.
2. Kurtz, S. M.; Muratoglu, O. K.; Evans, M.; Edidin, A. A. Biomaterials 1999, 20, 1659.
3. Goldmann, M.; Gronsky, R.; Pruitt, L. J Mater Sci Med 1998, 9, 207.
4. Becker, A.; Schmotzer, H.; Dirix, Y. Biomaterialien 2004, 5, 87.
5. Clegg, D.; Colleyer, A. Irradiation Effects on Polymers; Elsevier: New York, 1991.
6. Ivanoy, V. S. Radiation Chemistry of Polymers; VSP: Utrecht, 1992.
7. Shen, F. W.; Mc Kellop, H. A.; Salovey, R. J Polym Sci Part B: Polym Phys 1996, 34, 1063.
8. Zamfirova, G.; Pereña, J. M.; Benavente, R.; Pérez, E.; Cerrada, M. L.; Nedkov, E. Polym J 2002, 34, 125.
9. Stehling, F. C.; Mandelkern, L. Macromolecules 1970, 3, 242.
10. Matsuo, M.; Bin, Y.; Xu, C.; Ma, L.; Nakaoki, T.; Suzuki, T. Polymer 2003, 44, 4325.
11. Roy, S. K.; Kyu, T.; Manley, R. S. J. Macromolecules 1988, 21, 1741.
12. Yeh, J.-T.; Lin, Y.-T.; Chen, K.-N. J Polym Res 2003, 10, 55.
13. Boyd, R. H. Polym Eng Sci 1979, 19, 1010.
14. Hronský, V.; Murín, J.; Uhrin, J. Czech J Phys 2006, 56, 289.
15. McCrum, N. G.; Read, B. E.; Williams, G. Anelastic and Dielectric Effects in Polymeric Solids; Wiley: New York, 1967.
16. Boyd, R. H.; Yemni, T. Polym Eng Sci 1979, 19, 1023.
17. Hu, W.-G.; Schmidt-Rohr, K. Polymer 2000, 41, 2979.
18. Kawai, H.; Suehiro, S.; Shimomura, A. Polym Eng Rev 1983, 3, 109.
19. Abt, N. A.; Schneider, W.; Schön, R.; Riecker, C.B. In Crosslinked and Thermally Treated Ultra-High Molecular Weight Polyethylene for Joint Replacements; ASTM STP-Special Technical Publication; Kurtz, S. M.; Gsell, R.; Martell, J. Eds.; 2004, Issue 1445, 228.
20. ASTM. Standard Test Method for Evaluating *trans*-Vinylene Yield in Irradiated Ultra High Molecular-Weight Polyethylene Fabricated Forms Intended for Surgical Implants by Infrared Spectroscopy; ASTM International: West Conshohocken, PA, 2004.

21. ASTM. Standard Test Method for In Situ Determination of Network Parameters of Crosslinked Ultra-High Molecular Weight Polyethylene (UHMWPE); ASTM International: West Conshohocken, PA, 2002.
22. Flory, P.; Rehner, J. J Chem Phys 1943, 11, 521.
23. Trent, J. S.; Scheinbeim, J. I.; Couchman, P. R. Macromolecules 1983, 16, 589.
24. Bandrup, J.; Immergut, E. H. Polymer Handbook; Wiley: New York, 1989.
25. Hoffman, J. D.; Davies, G. T.; Lauritzen, J. J. I. In Treatise on Solid State Chemistry, Chapter 7: The Rate of Crystallization of Linear Polymers with Chain Folding; Hannay, N. B., Ed.; Plenum Press: New York, 1976, 3.
26. Strobl, G. The Physics of Polymers; Springer-Verlag: Berlin, 1997.
27. Cook, J. T. E.; Klein, P. G.; Ward, I. M.; Brain, A. A.; Farrar, D. F.; Rose, J. Polymer 2000, 41, 8615.
28. Farrar, D. F.; Brain, A. A. Biomaterials 1997, 18, 1677.
29. Nevoralová, M.; Baldrin, J.; Pospišil, J.; Chodák, I; Horák, Z. J Biomed Mater Res Part B: Appl Biomater 2005, 74, 800.
30. Stephens, C. P.; Benson, R. S.; Martinez-Pardo, M. E.; Barker, E. D.; Walker, J. B.; Stephens, T. P. Nucl Instrum Methods Phys Res Sect B 2005, 236, 540.
31. Zhao, Y.; Luo, Y. X.; Jiang, B. Z. J Appl Polym Sci 1993, 50, 1797.
32. Bartczak, Z.; Lezak, E. Polymer 2005, 46, 6050.
33. Göschel, U.; Ulrich, Ch. Crystallization of electron beam cross-linked UHMWPE. "PPS-24," Conference of the Polymer Processing Society, Salerno, Italy, 2008; Conf. Proc., paper S09–343.
34. Lewis, G. Biomaterials 2001, 22, 371.